

Wavy front dynamics in a three-component reaction-diffusion system with one activator and two inhibitors

E. P. Zemskov

Nonlinear Dynamics and Chaos Group, Physics Faculty, Moscow State University, 119992 Moscow, Russia

(Received 25 September 2005; revised manuscript received 6 February 2006; published 24 April 2006)

An analytic description for traveling waves in a one-dimensional reaction-diffusion system with one activator and two inhibitors and with equal diffusion constants is developed using a piecewise linear approximation for the nonlinear activator reaction term. The case of front waves is examined in more detail, the monotonic and oscillating fronts being separately considered. The corresponding wave profiles are constructed, and the speed equation is obtained and discussed. It is found that the fronts in the three-component model propagate faster than the fronts in the two-component system. The front interaction is studied using numerical calculations. The results show that at head-on collisions two oscillating fronts produce a wavy domain, which spreads in space with time.

DOI: [10.1103/PhysRevE.73.046127](https://doi.org/10.1103/PhysRevE.73.046127)

PACS number(s): 82.40.Ck, 02.50.Ey

I. PHYSICAL MOTIVATION

Reaction-diffusion (RD) equations generate spatial patterns in a variety of nonequilibrium systems [1–4]. Most of these systems is related to excitable media, where the wave propagation and interaction form spatial domains of different structure. Their features are revealed through analysis of the one-dimensional excitation waves as fronts and pulses. Such localized stationary and traveling solitary objects are basic fundamentals in many formation mechanisms [1]. The same structures are observed in chemical systems [2,3] and semiconductors [5]. Electrical pulses transmit the information in nervous systems of living objects [1]. Based on the work of Hodgkin and Huxley [6] nerve pulse conveying has been modeled by electrical transmission lines [7]. In this model the experimentally observed pulse propagation on the electrical system corresponds to localized solitary traveling solutions of a simple nonlinear two-component RD system of activator-inhibitor type with a cubic activator reaction term, the FitzHugh-Nagumo [7,8] system. Experimentally localized solitary objects are observed in planar gas-discharge systems with high Ohmic barrier as electrical current filaments [9]. A description of such patterns and more complex structures is given in Refs. [9,10].

Localized solitary objects in two-dimensional systems have been established as solutions of a three-component RD model [11]. These solutions were obtained by numerical integration in the following set [11]:

$$\begin{aligned} \frac{\partial u}{\partial t} &= f(u) - v - k_w w + k_0 + D_u \frac{\partial^2 u}{\partial x^2}, \\ \tau_v \frac{\partial v}{\partial t} &= u - v + D_v \frac{\partial^2 v}{\partial x^2}, \\ \tau_w \frac{\partial w}{\partial t} &= u - w + D_w \frac{\partial^2 w}{\partial x^2}, \end{aligned} \quad (1)$$

with a cubiclike nonlinear function $f(u) \sim u - u^3$ and positive parameters $\tau_{v,w}$ and $k_{w,0}$. This is the RD system

with one activator u and two inhibitors v, w . The inhibitors differ in their time $\tau_{v,w}$ and diffusion $D_{v,w}$ length scales. Under the action of an additional second inhibitor the localized solitary objects traveling on two-dimensional domains (spots) can be stabilized [11,12], because whereas the first inhibitor couples the dynamics of the leading front to the following back front [13,14], the second inhibitor stabilizes the shape of the wall of the activator in the directions perpendicular to the motion (lateral directions) of the spot [12].

From the point of view of gas-discharge physics, the activator is the current density in the gas, the first inhibitor is the voltage drop at a high Ohmic layer, the second inhibitor is related to temperature or another effective high Ohmic layer, $f(u)$ is the voltage current characteristic of gas, $\tau_{v,w}$ are the dielectric relaxation time, k_0 is the applied voltage, and k_w is the strength of influence of inhibitor on $\partial u / \partial t$ [10].

An analytic treatment of RD equations is possible when the nonlinear reaction term is approximated by a piecewise linear function. This approach, well known in the literature since 1970 [15], allows us to obtain analytic solutions for the propagating waves. The method has more general applicability and is often the only way to investigate some nonlinear problems analytically in an approximate fashion [16]. In the last decade, piecewise linear models have been widely employed to use the translational invariance of equations as a speed selection mechanism [17,18], to study the effect of transport memory [19–21] and the wave propagation in discrete [22,23] and inhomogeneous [24] media, and to consider a forcing influence [25]. In most papers related to RD equations, one-component [15,17,19,20,25–27] and two-component [13,18,28–32] systems are investigated so that, to the best of our knowledge, before the present study, no fully analytic solutions for the traveling waves in the three-component RD systems were available. Thus, the main problem statement for present work is the analytic description of fronts in the piecewise linear system.

II. FACTORIZATION OF THE CHARACTERISTIC EQUATION

The starting position is a one-dimensional three-component RD system with one activator $u(x,t)$ and two inhibitors $v(x,t)$ and $w(x,t)$ [10–12],

$$\begin{aligned}\frac{\partial u}{\partial t} &= f(u) - v - w + D_u \frac{\partial^2 u}{\partial x^2}, \\ \frac{\partial v}{\partial t} &= \varepsilon u - \beta v + D_v \frac{\partial^2 v}{\partial x^2}, \\ \frac{\partial w}{\partial t} &= \varepsilon^* u - \beta^* w + D_w \frac{\partial^2 w}{\partial x^2},\end{aligned}\quad (2)$$

with steplike initial conditions

$$u(x,0) = u_0 \chi(x), \quad v(x,0) = v_0 \chi(x), \quad w(x,0) = w_0 \chi(x), \quad (3)$$

where $\chi(x) = 2\theta(x-x_0) - 1$ and u_0, v_0, w_0 , and x_0 are constant. These initial conditions describe a localized perturbation at $x=x_0$ in the form of a front solution of steplike shape.

In Eq. (2) the cubic activator reaction term $f(u) \sim u - u^3$ is approximated by a piecewise linear function $f(u) = -\alpha u - 1 + 2\theta(u) \equiv -\alpha u \mp 1$, where $\theta(u)$ is the Heaviside step function; positive parameters $\varepsilon, \varepsilon^*, \beta$, and β^* represent the ratios of the time scales on which u, v , and w vary. In contrast to the well-known two-component Rinzel-Keller model [33], in which the slope of pieces $\alpha=1$, in presented model one can change this positive parameter, which allows one to find the exact solutions. In present paper, the consideration is restricted to the case of equal diffusion constants $D_u = D_v = D_w = 1$. In the situation with different diffusion constants the system is exactly solvable for the stationary case when $\partial u / \partial t = \partial v / \partial t = \partial w / \partial t = 0$.

The inhibitors are coupled in the model by the activator equation. This coupling becomes more visible when a new variable $\hat{v} = v + w$ is introduced. Then summarizing of the inhibitor equations the model system (with equal diffusion constants) reads

$$\begin{aligned}\frac{\partial u}{\partial t} &= f(u) - \hat{v} + \frac{\partial^2 u}{\partial x^2}, \\ \frac{\partial \hat{v}}{\partial t} &= (\varepsilon + \varepsilon^*)u - \beta \hat{v} - (\beta^* - \beta)w + \frac{\partial^2 \hat{v}}{\partial x^2}, \\ \frac{\partial w}{\partial t} &= \varepsilon^* u - \beta^* w + \frac{\partial^2 w}{\partial x^2}.\end{aligned}\quad (4)$$

When $\beta = \beta^*$ the first and second equations present an isolated two-component system. Thus, to obtain new nontrivial (related to the two-component model) results we must consider the case $\beta \neq \beta^*$.

Introducing the traveling frame coordinate $\xi = x - ct$, where c is the wave velocity, Eq. (2) can be rewritten for the propagating solutions $u(\xi), v(\xi)$, and $w(\xi)$ as

$$\frac{d^2 u}{d\xi^2} + c \frac{du}{d\xi} - \alpha u - v - w \mp 1 = 0,$$

$$\frac{d^2 v}{d\xi^2} + c \frac{dv}{d\xi} + \varepsilon u - \beta v = 0,$$

$$\frac{d^2 w}{d\xi^2} + c \frac{dw}{d\xi} + \varepsilon^* u - \beta^* w = 0. \quad (5)$$

The method of finding the traveling-wave solutions is very simple: thanks to the piecewise linear character of the rate function $f(u)$, the solution for each piece satisfies a linear equation. The one-piece solution may then be expressed as a superposition of six exponentials,

$$\begin{aligned}u(\xi) &= \sum_{n=1}^6 A_n e^{\lambda_n \xi} + \bar{u}, \quad v(\xi) = \sum_{n=1}^6 B_n e^{\lambda_n \xi} + \bar{v}, \\ w(\xi) &= \sum_{n=1}^6 B_n^* e^{\lambda_n \xi} + \bar{w},\end{aligned}\quad (6)$$

where A_n, B_n , and B_n^* are integration constants to be determined in each of the regions $u < 0$ and $u > 0$; the parameters $\bar{u}, \bar{v}, \bar{w} = \text{const}$ represent the coordinates of the fixed points. Inserting Eqs. (6) into Eqs. (5) and collecting the terms proportional to $e^{\lambda_n \xi}$, we obtain the matrix equation $\mathbf{GH} = 0$ with

$$\mathbf{G} = \begin{pmatrix} \gamma - \alpha & -1 & -1 \\ \varepsilon & \gamma - \beta & 0 \\ \varepsilon^* & 0 & \gamma - \beta^* \end{pmatrix}, \quad \mathbf{H} = \begin{pmatrix} A \\ B \\ B^* \end{pmatrix}. \quad (7)$$

Here the notation $\gamma = \lambda_n^2 + c\lambda_n$ is introduced. The determinant of the matrix \mathbf{G} is equal to zero when

$$(\gamma - \alpha)(\gamma - \beta)(\gamma - \beta^*) + \varepsilon^*(\gamma - \beta) + \varepsilon(\gamma - \beta^*) = 0. \quad (8)$$

This cubic equation may be easily factorized for some values of the parameter α : if it is chosen as

$$\alpha = \frac{\varepsilon \beta^* + \varepsilon^* \beta}{\varepsilon + \varepsilon^*}, \quad (9)$$

then $\varepsilon^*(\gamma - \beta) + \varepsilon(\gamma - \beta^*) = (\varepsilon + \varepsilon^*)(\gamma - \alpha)$ and Eq. (8) becomes

$$(\gamma - \alpha)[(\gamma - \beta)(\gamma - \beta^*) + \varepsilon + \varepsilon^*] = 0, \quad (10)$$

so that its roots read

$$\gamma_0 = \alpha, \quad \gamma_{1,2} = \frac{\beta + \beta^*}{2} \pm \sqrt{\frac{(\beta - \beta^*)^2}{4} - \varepsilon - \varepsilon^*}. \quad (11)$$

Hence the eigenvalues

$$\begin{aligned}\lambda_{1,2} &= -c/2 \pm \sqrt{c^2/4 + \gamma_0} \equiv -c/2 \pm \nu_0, \\ \lambda_{3,4} &= -c/2 \pm \sqrt{c^2/4 + \gamma_1} \equiv -c/2 \pm \nu_1, \\ \lambda_{5,6} &= -c/2 \pm \sqrt{c^2/4 + \gamma_2} \equiv -c/2 \pm \nu_2;\end{aligned}\quad (12)$$

the integration constants B_n and B_n^* can be expressed as

$$\begin{aligned}
 B_{1,2} &= b_0 A_{1,2}, & B_{3,4} &= b_1 A_{3,4}, & B_{5,6} &= b_2 A_{5,6}, \\
 B_{1,2}^* &= -b_0 A_{1,2}, & B_{3,4}^* &= b_1^* A_{3,4}, & B_{5,6}^* &= b_2^* A_{5,6}
 \end{aligned} \quad (13)$$

with

$$b_m = \frac{\varepsilon}{\beta - \gamma_m}, \quad b_m^* = \frac{\varepsilon^*}{\beta^* - \gamma_m}, \quad m = 0, 1, 2. \quad (14)$$

Thus, the model contains in fact four parameter ε , β , ε^* , and β^* ; the α parameter is just their combination determined by Eq. (9). All four parameters present the ratios between the time scales associated with the two field pairs, u/v and u/w . When $\varepsilon = \beta$ for the two-component model is chosen [34] the general case is modelled by some other constants. In present paper two additional time scales β and β^* are also introduced for generality. The physical meaning of the choices and restrictions on the parameters are related to the context of excitable media, where $\varepsilon, \beta \ll 1$. As follows from the general theory of excitation waves [35] dissipative structures (in particular, static, pulsating, and traveling waves) may in principle coexist when the system parameters lie between some narrow regions, in particular when $0 < \varepsilon \ll 1$ and $0 < \beta \ll 1$. In presented paper the typical values $\varepsilon, \beta \sim 0.1$ are chosen.

III. DESCRIPTION OF THE FRONTS

In this section one specific type of the traveling-wave solutions, the front solution, is examined in more detail. The fronts present two-piece waves connecting two different fixed points at $\xi \rightarrow -\infty$ and $\xi \rightarrow +\infty$, respectively.

A. Monotonic fronts

Since the constants ε , β , ε^* , β^* , and α are positive, the eigenvalues $\lambda_{1,3,5} > 0$ and $\lambda_{2,4,6} < 0$. Here we consider the case when $(\beta - \beta^*)^2/4 \geq \varepsilon + \varepsilon^*$. When $(\beta - \beta^*)^2/4 < \varepsilon + \varepsilon^*$ the eigenvalues λ_{3-6} and constants B_{3-6} become imaginary and the solutions $u(\xi)$, $v(\xi)$, and $w(\xi)$ contain cosine and sine terms. This situation will be considered later.

Taking into account the signs of λ_n Eqs. (12) the construction of the fronts reads

$$\begin{aligned}
 u_1(\xi) &= A_1 e^{\lambda_1 \xi} + A_3 e^{\lambda_3 \xi} + A_5 e^{\lambda_5 \xi} - s, & \xi \leq 0, \\
 u_2(\xi) &= A_2 e^{\lambda_2 \xi} + A_4 e^{\lambda_4 \xi} + A_6 e^{\lambda_6 \xi} + s, & \xi \geq 0, \\
 v_1(\xi) &= B_1 e^{\lambda_1 \xi} + B_3 e^{\lambda_3 \xi} + B_5 e^{\lambda_5 \xi} - r, & \xi \leq 0, \\
 v_2(\xi) &= B_2 e^{\lambda_2 \xi} + B_4 e^{\lambda_4 \xi} + B_6 e^{\lambda_6 \xi} + r, & \xi \geq 0, \\
 w_1(\xi) &= B_1^* e^{\lambda_1 \xi} + B_3^* e^{\lambda_3 \xi} + B_5^* e^{\lambda_5 \xi} - r^*, & \xi \leq 0, \\
 w_2(\xi) &= B_2^* e^{\lambda_2 \xi} + B_4^* e^{\lambda_4 \xi} + B_6^* e^{\lambda_6 \xi} + r^*, & \xi \geq 0,
 \end{aligned} \quad (15)$$

where

$$s = 1/(\alpha + \varepsilon/\beta + \varepsilon^*/\beta^*), \quad r = (\varepsilon/\beta)s, \quad r^* = (\varepsilon^*/\beta^*)s \quad (16)$$

are the coordinates of the fixed points. Both parts of these solutions are patched together using the matching conditions

for functions and their derivatives at $\xi=0$; i.e., there are six equations for u , v , w , $du/d\xi$, $dv/d\xi$, and $dw/d\xi$, the seventh equation having its origin in $u(\xi=0)=0$. Thus, we have

$$\begin{aligned}
 A_1 + A_3 + A_5 - s &= A_2 + A_4 + A_6 + s, \\
 A_1 \lambda_1 + A_3 \lambda_3 + A_5 \lambda_5 &= A_2 \lambda_2 + A_4 \lambda_4 + A_6 \lambda_6, \\
 A_1 + A_3 + A_5 - s &= 0, \\
 B_1 + B_3 + B_5 - r &= B_2 + B_4 + B_6 + r, \\
 B_1 \lambda_1 + B_3 \lambda_3 + B_5 \lambda_5 &= B_2 \lambda_2 + B_4 \lambda_4 + B_6 \lambda_6, \\
 B_1^* + B_3^* + B_5^* - r^* &= B_2^* + B_4^* + B_6^* + r^*, \\
 B_1^* \lambda_1 + B_3^* \lambda_3 + B_5^* \lambda_5 &= B_2^* \lambda_2 + B_4^* \lambda_4 + B_6^* \lambda_6.
 \end{aligned} \quad (17)$$

From these seven equations it is easy to obtain after simple mathematics six expressions for the A_n constants and the speed equation. The results are

$$\begin{aligned}
 A_1 &= s + \frac{q_2}{\hat{b}v_1} \lambda_4 - \frac{q_1}{\hat{b}v_2} \lambda_6, \\
 A_2 &= -s + \frac{q_2}{\hat{b}v_1} \lambda_3 - \frac{q_1}{\hat{b}v_2} \lambda_5, \\
 A_3 &= -\frac{q_2}{\hat{b}v_1} \lambda_4, \\
 A_4 &= -\frac{q_2}{\hat{b}v_1} \lambda_3, \\
 A_5 &= \frac{q_1}{\hat{b}v_2} \lambda_6, \\
 A_6 &= \frac{q_1}{\hat{b}v_2} \lambda_5,
 \end{aligned} \quad (18)$$

$$\begin{aligned}
 q_1 &= (b_1 + b_1^*)(r - b_0 s) + (b_0 - b_1)(r + r^*), \\
 q_2 &= (b_2 + b_2^*)(r - b_0 s) + (b_0 - b_2)(r + r^*), \\
 \hat{b} &= (b_1 + b_1^*)(b_0 - b_2) + (b_2 + b_2^*)(b_1 - b_0);
 \end{aligned} \quad (19)$$

the speed equation reads

$$c[(q_1 - q_2 + s\hat{b})v_1 v_2 - v_0(q_1 v_1 - q_2 v_2)] = 0. \quad (20)$$

From the speed equation it follows that there exists a trivial solution $c=0$, a stationary front. Other solutions describe two counterpropagating fronts with positive and negative velocities because Eq. (20) is symmetrical under the transformation $c \rightarrow -c$ due to $v_m^2 \propto c^2$, $m=0, 1, 2$. Since $q_{1,2} \propto s$, all solutions

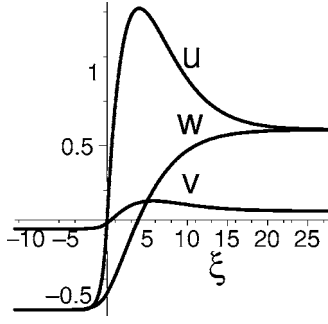


FIG. 1. Front profiles $u=u(\xi)$, $v=v(\xi)$, and $w=w(\xi)$ for $\varepsilon=\varepsilon^*=\beta^*=0.1$ and $\beta=1$. The value of the front speed is $c \approx -1.05$.

are independent of variations of the fixed-point coordinates s , r , and r^* .

An example of the front profiles $u=u(\xi)$, $v=v(\xi)$, and $w=w(\xi)$ for typical [with the exception of $\beta=1$, this value is chosen only for illustrative purposes to show the monotonic fronts; otherwise, the front becomes oscillatory (see the next section, Sec. III B)] for excitable media values ($\varepsilon=\varepsilon^*=\beta^*=0.1$) of the time-scale parameters as illustrated in Fig. 1. As expected, the ratio of the time scales reflects the difference between the front profiles of activator and inhibitor so that the u and w profiles resemble to the corresponding (activator and inhibitor, respectively) front curves in the two-component system [34], whereas the v profile repeats the u wave on a reduced scale at $\varepsilon < \beta$. When $\varepsilon \rightarrow \beta$ the v curve grows and tends to the u profile so that for $\varepsilon > \beta$ the v front is larger than the u wave.

The fronts displayed in Fig. 1 propagate with negative velocities—i.e., from the right to left side in Fig. 1. However, it has been found that there also exists fronts with zero and positive velocities at the same values of the model param-

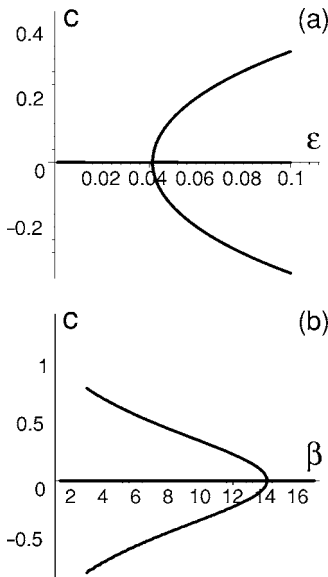


FIG. 2. Speed diagrams $c=c(\varepsilon, \beta)$ for fixed (a) $\beta=10$ and (b) $\varepsilon=0.1$. The values of the time-scale parameters for the second inhibitor are fixed at $\varepsilon^*=\beta^*=0.1$.

eters. This fact can be generalized to a speed diagram. This diagram (Fig. 2) is derived using the speed equation (20) for fixed β [Fig. 2(a)] or ε [Fig. 2(b)]. The speed curve has the trivial solution $c=0$ in addition to the two symmetric branches which bifurcate at some critical values of the varied parameter. Note the qualitative similarity with the nonequilibrium Ising-Bloch bifurcation found in the two-component system [34,36]. The difference is quantitative: the bifurcation point in the two-component system occurs at $\varepsilon=\beta < 0.4$ for positive α , as follows for ε_{cr} in Eq. (3.4) and Fig. 3 in Ref. [36], whereas the bifurcation in the three-component model appears at the nontypical (for excitable media) values of ε and β .

B. Oscillating fronts

Special consideration must be given to waves with oscillating tails. Traveling waves with spatial oscillations in profiles were described in different RD systems [20,23,36]. In the present research, as noted above in Sec. III A, when $(\beta-\beta^*)^2/4 < \varepsilon+\varepsilon^*$ the eigenvalues λ_{3-6} are imaginary due to

$$\gamma_{1,2} = \frac{\beta + \beta^*}{2} \pm i \sqrt{\varepsilon + \varepsilon^* - \frac{(\beta - \beta^*)^2}{4}} \equiv \frac{\beta + \beta^*}{2} \pm ip, \quad i^2 = -1, \quad (21)$$

i.e.,

$$\lambda_{3,4} = -\frac{c}{2} \pm \sqrt{\frac{c^2}{4} + \frac{\beta + \beta^*}{2}} + ip = -\frac{c}{2} \pm y \pm iz, \quad \lambda_{5,6} = -\frac{c}{2} \pm \sqrt{\frac{c^2}{4} + \frac{\beta + \beta^*}{2}} - ip = -\frac{c}{2} \pm y \mp iz, \quad (22)$$

where

$$y = \sqrt{\frac{1}{2}(\sqrt{c_\beta^2 + p^2} + c_\beta)}, \quad z = \sqrt{\frac{1}{2}(\sqrt{c_\beta^2 + p^2} - c_\beta)}, \quad c_\beta = \frac{c^2}{4} + \frac{\beta + \beta^*}{2} \quad (23)$$

are positive quantities and $y > c/2$ so that the real parts of the parameters $\lambda_{3,5}$ are positive and the real parts of $\lambda_{4,6}$ are negative. These expressions are similar to the case of the two-component system [36]. Hence the front solutions read

$$u_1(\xi) = A_1 e^{\lambda_1 \xi} + e^{(-c/2+y)\xi} [A_3 \cos(z\xi) + A_5 \sin(z\xi)] - s,$$

$$\xi \leq 0,$$

$$u_2(\xi) = A_2 e^{\lambda_2 \xi} + e^{(-c/2-y)\xi} [A_4 \cos(z\xi) + A_6 \sin(z\xi)] + s,$$

$$\xi \geq 0,$$

$$v_1(\xi) = B_1 e^{\lambda_1 \xi} + e^{(-c/2+y)\xi} [B_3 \cos(z\xi) + B_5 \sin(z\xi)] - r,$$

$$\xi \leq 0,$$

$$\begin{aligned}
 v_2(\xi) &= B_2 e^{\lambda_2 \xi} + e^{(-c/2-y)\xi} [B_4 \cos(z\xi) + B_6 \sin(z\xi)] + r, \\
 \xi &\geq 0, \\
 w_1(\xi) &= B_1^* e^{\lambda_1 \xi} + e^{(-c/2+y)\xi} [B_3^* \cos(z\xi) + B_5^* \sin(z\xi)] - r^*, \\
 \xi &\leq 0, \\
 w_2(\xi) &= B_2^* e^{\lambda_2 \xi} + e^{(-c/2-y)\xi} [B_4^* \cos(z\xi) + B_6^* \sin(z\xi)] + r^*, \\
 \xi &\geq 0.
 \end{aligned}
 \tag{24}$$

Here B_n and B_n^* constants are functions of the A_n constants:

$$\begin{aligned}
 B_{3,5} &= \frac{\varepsilon}{\varepsilon + \varepsilon^*} \left(\frac{\beta - \beta^*}{2} A_{3,5} \pm pA_{5,3} \right), \\
 B_{4,6} &= \frac{\varepsilon}{\varepsilon + \varepsilon^*} \left(\frac{\beta - \beta^*}{2} A_{4,6} \mp pA_{6,4} \right), \\
 B_{3,5}^* &= \frac{\varepsilon^*}{\varepsilon + \varepsilon^*} \left(-\frac{\beta - \beta^*}{2} A_{3,5} \pm pA_{5,3} \right), \\
 B_{4,6}^* &= \frac{\varepsilon^*}{\varepsilon + \varepsilon^*} \left(-\frac{\beta - \beta^*}{2} A_{4,6} \mp pA_{6,4} \right),
 \end{aligned}
 \tag{25}$$

$B_{1,2}$ and $B_{1,2}^*$ constants being determined by Eq. (13). The A_n constants and the front speed c are derived from the matching procedure as was done in the case of monotonic fronts. The front profiles obtained, $u, v, w(\xi)$, are shown in Fig. 3(a). For simplicity, the parameters of the inhibitor reaction functions are chosen as $\varepsilon = \beta$ and $\varepsilon^* = \beta^*$. Since the situation with $\beta \neq \beta^*$ is considered, the time scales are set to $\varepsilon > \varepsilon^*$ for the sake of definiteness so that the v and w inhibitors are strong and weak, respectively.

It is instructive to compare here the front behavior in the three-component model with fronts in the two-component systems with the same parameter values—i.e., with 2 two-component systems, where the first one is with strong and the second one is with weak inhibitors, separately. These models are described by following equations:

$$\begin{aligned}
 \frac{\partial u}{\partial t} &= f(u) - \tilde{v} + \frac{\partial^2 u}{\partial x^2}, \\
 \frac{\partial \tilde{v}}{\partial t} &= \tilde{\varepsilon}(u - \tilde{v}) + \frac{\partial^2 \tilde{v}}{\partial x^2},
 \end{aligned}
 \tag{26}$$

with $\tilde{v} = v$, $\tilde{\varepsilon} = \varepsilon$ and $\tilde{v} = w$, $\tilde{\varepsilon} = \varepsilon^*$ for the models with strong and weak inhibitors, respectively. The piecewise linear function $f(u)$ is the same as in Eq. (2). Exact analytic solutions for monotonic and oscillating fronts in the activator-inhibitor system of this type were obtained earlier [36].

The comparison of the three- and two-component cases is presented graphically in Fig. 3. Results for the models with strong and weak inhibitors are shown in Figs. 3(b) and 3(c), respectively. It can be seen that the front profiles in the three-

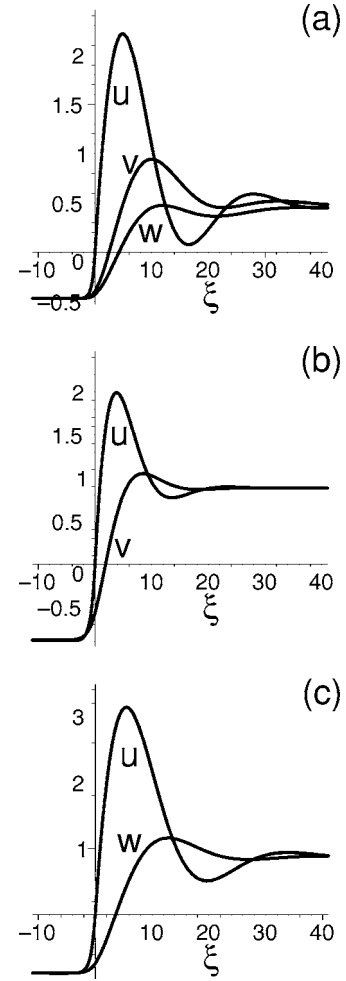


FIG. 3. Profiles $u=u(\xi)$, $v=v(\xi)$, and $w=w(\xi)$ for fronts (a) in the three-component system with $\varepsilon = \beta = 0.2$ and $\varepsilon^* = \beta^* = 0.1$ and in the two-component systems with (b) strong inhibitor, where $\varepsilon = \beta = 0.2$ and with (c) weak inhibitor, where $\varepsilon^* = \beta^* = 0.1$. The values of the front speed are (a) $c \approx -1.77$, (b) $c \approx -0.93$, and (c) $c \approx -1.17$. The value of α is the same for all three cases.

component system (3-fronts) differ quantitatively from the fronts in the two-component systems (2-fronts). Moreover, the 3-front is not a superposition of both 2-fronts. It is remarkable that the speed value of the 3-front is larger than any 2-front velocity. This fact seems unexpected, but may be explained as follows. It is known [10,12] that the second inhibitor is introduced to stabilize two-dimensional domains. In presented research all diffusion constants are equal. Therefore both inhibitors couple the dynamics of the front and back with similar effect. Hence the pattern is localized better with clearly delineated boundary (less smeared) than the domain for the model with one inhibitor; i.e., the shape becomes steeper. And the steep wave propagates faster than the sloping one. For the fronts depicted in Fig. 3 this means that the wave with more pronounced oscillations (a) travels faster than the waves with slightly oscillating tails (b), (c).

IV. FRONT INTERACTION

Further properties of fronts are determined here using numerical calculations for three- and two-component systems.

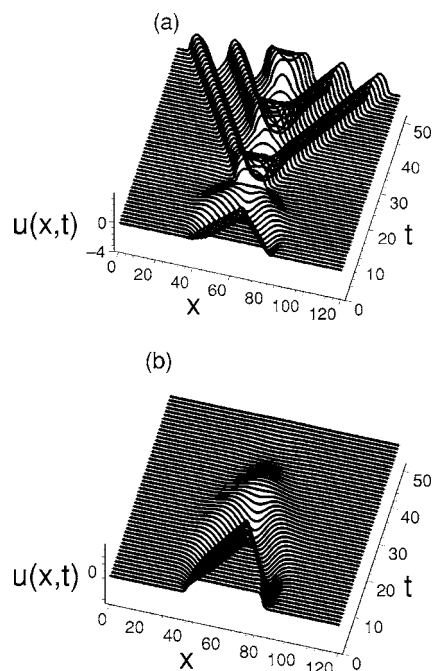


FIG. 4. Front-back interactions. Three-dimensional diagrams $u(x,t)$ versus x and t starting from step initial conditions are shown for (a) three-component and (b) two-component systems in the case of the nonsymmetric piecewise linear function $f(u) = -\alpha u - 1 + 2\theta(u - u_0)$ with $u_0 = 0.1$. All parameters are chosen as for Fig. 3: (a) $\varepsilon = \beta = 0.2$, $\varepsilon^* = \beta^* = 0.1$ and (b) $\varepsilon^* = \beta^* = 0.1$ (weak inhibitor). The finite-difference scheme with zero-flux conditions at both boundaries is employed for numeric integration. The grid values are fixed at $\Delta x = 0.1$, $N_x = 1, 2, \dots, 1200$ and $\Delta t = 0.001$, $N_t = 1, 2, \dots, 50000$ so that $x = 120$ and $t = 50$.

These properties are related to the nonlinear dynamics of the front interaction, and therefore it is difficult to describe them analytically [37]. To study the interaction dynamics an equation of motion for a pair of colliding waves was derived by the interfacial approach [38]. In the present research the head-on collision effect of the interacting fronts has come about through the appropriate choice of initial conditions and the nonsymmetric activator reaction function $f(u) = -\alpha u - 1 + 2\theta(u - u_0)$ with $u_0 = 0.1$; two square steps present the front and back for the initial data.

In Fig. 4 an example of the front collisions is shown. For the two-component system the colliding fronts annihilate [Fig. 4(b)], whereas for the three-component model they produce a wavy pattern [Fig. 4(a)] that spreads in an oscillatory manner. This pattern is formed by the repetition of two counterpropagating waves and is initiated by the collision of oscillating tails as if they are elastic objects even in dissipative

systems. Colliding traveling waves in the three-component system with one activator and two inhibitors are repulsive near a bifurcation point; in fact, they scatter during collisions [39]. This phenomenon is similar to the periodic wave-train generation in oscillatory RD equations [40]. However, in the present system the bistable dynamics is realized and hence the following conclusion can be reached. The origin of this effect is due to the intersection of two features: the second inhibitor and the oscillating front. When there is no second inhibitor (i.e., in the case of the two-component system) or otherwise when the front in the three-component system is monotonic, the colliding front and back annihilate. This is valid for the two-component system with any (strong or weak) inhibitor.

V. SUMMARY

The exact analytic solutions for traveling waves in the three-component reaction-diffusion system of the activator-inhibitor type were derived. The propagating fronts were explicitly written and the integration constants were found from a set of transcendental equations, which were compactly solved within any power of the smallness of the time-scale parameters. Two type of fronts, monotonic and oscillating, were considered and their speeds calculated. It was found that the front in the three-component model propagates faster than the front in the two-component system. The front interaction was investigated using numerical calculations. These studies showed that during collisions of the oscillating fronts a wavy pattern was initiated. The pattern is formed by the repetition of two counterpropagating waves and spreads with time and resembles the periodic wave train due to spatial oscillations. The wavy domain occurs only for colliding *oscillatory* fronts in the *three-component* system.

In the present research both analytic and numerical methods were used for studies of the problem of front propagation and interaction in the reaction-diffusion system. The model with inverted N type of activator reaction function was applied to the cubic nonlinearity. However, the piecewise linear approximation can be made for systems with more complicated nonlinear reaction terms [26], leading to a generalization to multistable cases [41], which may be considered in the context of the above-described approach.

ACKNOWLEDGMENTS

Part of the results presented in Sec. II were obtained in collaboration with Professor Klaus Kassner from Otto-von-Guericke-University in Magdeburg (Germany), to whom author is very grateful.

- [1] J. D. Murray, *Mathematical Biology*, 3rd ed. (Springer-Verlag, Berlin, 2003).
 [2] *Chemical Waves and Patterns*, edited by R. Kapral and K. Showalter (Kluwer, Dordrecht, 1995).

- [3] M. C. Cross and P. C. Hohenberg, *Rev. Mod. Phys.* **65**, 851 (1993).
 [4] E. Meron, *Phys. Rep.* **218**, 1 (1992).
 [5] E. Schöll, *Nonlinear Spatio-temporal Dynamics and Chaos in*

- Semiconductors* (Cambridge University Press, Cambridge, England, 2001).
- [6] A. L. Hodgkin and A. F. Huxley, *J. Physiol. (London)* **117**, 500 (1952).
- [7] J. Nagumo, S. Arimoto, and S. Yoshizawa, *Proc. IRE* **50**, 2061 (1962).
- [8] R. FitzHugh, *Biophys. J.* **1**, 445 (1961).
- [9] H.-G. Purwins, Y. Astrov, and I. Brauer, in *Proceedings of Fifth Experimental Chaos Conference 1999*, edited by M. Ding, W. L. Ditto, L. M. Pecora, and M. L. Spano (World Scientific, Singapore, 2001), pp. 3–13.
- [10] M. Bode, A. W. Liehr, C. P. Schenk, and H.-G. Purwins, *Physica D* **161**, 45 (2002).
- [11] C. P. Schenk, M. Or-Guil, M. Bode, and H.-G. Purwins, *Phys. Rev. Lett.* **78**, 3781 (1997).
- [12] M. Or-Guil, M. Bode, C. P. Schenk, and H.-G. Purwins, *Phys. Rev. E* **57**, 6432 (1998).
- [13] J. Rinzel and D. Terman, *SIAM J. Appl. Math.* **42**, 1111 (1982).
- [14] P. Ortoleva and J. Ross, *J. Chem. Phys.* **63**, 3398 (1975).
- [15] H. P. McKean, *Adv. Math.* **4**, 209 (1970).
- [16] S. Theodorakis, *Phys. Rev. D* **60**, 125004 (1999).
- [17] S. Theodorakis and E. Leontidis, *Phys. Rev. E* **62**, 7802 (2000).
- [18] S. Theodorakis and E. Leontidis, *Phys. Rev. E* **65**, 026122 (2002).
- [19] V. Méndez and J. E. Llebot, *Phys. Rev. E* **56**, 6557 (1997); V. Méndez and A. Compte, *Physica A* **260**, 90 (1998).
- [20] K. K. Manne, A. J. Hurd, and V. M. Kenkre, *Phys. Rev. E* **61**, 4177 (2000).
- [21] G. Abramson, A. R. Bishop, and V. M. Kenkre, *Phys. Rev. E* **64**, 066615 (2001).
- [22] A. Tonnelier, *Phys. Rev. E* **67**, 036105 (2003).
- [23] A. Carpio and L. L. Bonilla, *Phys. Rev. E* **67**, 056621 (2003); A. Carpio, *ibid.* **69**, 046601 (2004).
- [24] A. Prat and Y.-X. Li, *Physica D* **186**, 50 (2003); A. Prat, Y.-X. Li, and P. Bressloff, *ibid.* **202**, 177 (2005); V. Méndez, J. Fort, H. G. Rotstein, and S. Fedotov, *Phys. Rev. E* **68**, 041105 (2003).
- [25] R. Bakanas, *Phys. Rev. E* **69**, 016103 (2004); **71**, 026201 (2005).
- [26] U. Ebert and W. van Saarloos, *Physica D* **146**, 1 (2000).
- [27] R. Bakanas, *Nonlinearity* **16**, 313 (2003).
- [28] A. Ito and T. Ohta, *Phys. Rev. A* **45**, 8374 (1992).
- [29] S. Koga, *Physica D* **84**, 148 (1995).
- [30] E. M. Kuznetsova and V. V. Osipov, *Phys. Rev. E* **51**, 148 (1995).
- [31] Y. B. Chernyak, J. M. Starobin, and R. J. Cohen, *Phys. Rev. Lett.* **80**, 5675 (1998).
- [32] C. B. Muratov and V. V. Osipov, *Physica D* **155**, 112 (2001); *SIAM J. Appl. Math.* **62**, 1463 (2002).
- [33] J. Rinzel and J. B. Keller, *Biophys. J.* **13**, 1313 (1973).
- [34] A. Hagberg and E. Meron, *Nonlinearity* **7**, 805 (1994); *Phys. Rev. E* **48**, 705 (1993).
- [35] B. S. Kerner and V. V. Osipov, *Autosolitons: a New Approach to Problem of Self-Organization and Turbulence* (Kluwer, Boston, 1994); *Usp. Fiz. Nauk* **157**, 201 (1989) [*Sov. Phys. Usp.* **32**, 101 (1989)].
- [36] E. P. Zemskov, V. S. Zykov, K. Kassner, and S. C. Müller, *Nonlinearity* **13**, 2063 (2000).
- [37] M. Sheintuch and O. Nekhamkina, *Phys. Rev. E* **63**, 056120 (2001).
- [38] T. Ohta, J. Kiyose, and M. Mimura, *J. Phys. Soc. Jpn.* **66**, 1551 (1997).
- [39] Y. Nishiura, T. Teramoto, and K.-I. Ueda, *Phys. Rev. E* **67**, 056210 (2003).
- [40] J. A. Sherratt, *SIAM J. Appl. Math.* **63**, 1520 (2003); A. Tonnelier, *ibid.* **63**, 459 (2002); O. Descalzi, Y. Hayase, and H. R. Brand, *Phys. Rev. E* **69**, 026121 (2004).
- [41] E. P. Zemskov, *Phys. Rev. E* **69**, 036208 (2004).